ELSEVIER

Catalysis Today 23 (1995) 371–377

CATALYSIS TODAY

CO and NO chemisorption on heavy metal surfaces: cluster model study

Noriko Watari [a,*], Shuhei Ohnishi [b]

[a] *NEC Informatec Systems, Ltd., KSP R&D Bldg., Sakado 3-2-1 Takatsu-ku, Kawasaki, Kanagawa 213, Japan*

[b] *NEC Fundamental Research Labs., Miyukigaoka 34, Tsukuba, Ibaraki 305, Japan*

Abstract

The mechanism for CO or NO strong and weak chemisorptions on tungsten and platinum surfaces is discussed by the cluster model for metal surfaces on the basis of the local density functional scheme using the norm-conserving pseudo-potential in the linear combination of atomic orbitals method. Total energies, stretching frequencies and electronic structures of adsorbed CO and NO molecules obtained by the self-consistent calculations provide us with information to understand the experimental phenomena quantitatively.

1. Calculation method

1.1. LCPSAO method

The LCPSAO method for the electronic structure calculation of the finite atomic system is characterized by the introduction of two effective model potentials, the norm-conserving pseudo-potential and the non-local bulk-like potential of embedded type, into the standard linear combination of atomic orbitals (LCAO) scheme, whose details were described in our previous work [1]. The total Hamiltonian for the present system is written as follows:

$$H=\left[-\frac{1}{2}\nabla^2+\sum_{il}\hat{V}_{il}^{\mathrm{ps}}(\mathbf{r}-\mathbf{R}_i)+V_{\mathrm{val}}(\mathbf{r})+\hat{V}_{\mathrm{ext}}\right] \quad (1)$$

where $\mathbf{R}_i$ is the atomic site, $\hat{V}_{il}^{\mathrm{ps}}$ is the effective core pseudo-potential for the atom located at the site $\mathbf{R}_i$. The norm-conserving pseudo-potential is given by the sum of the long-range core potential $V_{\mathrm{core}}(\mathbf{r})$ and the non-local angular-momentum-dependent potential $\hat{V}_l^{\mathrm{ion}}(\mathbf{r})$ [2]. V_{val} is the sum of Coulomb potential, V_{C}, and the exchange-correlation potential, V_{XC}, given by $V_{\mathrm{XC}}(\mathbf{r})=\partial E_{\mathrm{XC}}/\partial\rho(\mathbf{r})$ [3], where $E_{\mathrm{XC}}[\rho]$ is the exchange-correlation energy. $\rho(\mathbf{r})$ is the electron density. The external model potential $\hat{V}_{\mathrm{ext}}$ is defined as the sum of the effective model potential $\hat{V}_{\mathrm{M}}$ located on the cluster-surrounding atoms. $\hat{V}_{\mathrm{M}}$ is constructed by the following formula,

$$\hat{V}_{\mathrm{M}}=\sum_{\kappa,i}\frac{V_{\mathrm{loc},i}|\Phi_{\kappa,i}><\Phi_{\kappa,i}|V_{\mathrm{loc},i}}{<\Phi_{\kappa,i}|V_{\mathrm{loc},i}|\Phi_{\kappa,i}>} \quad (2)$$

where $V_{\mathrm{loc},i}$ is the embedded local potential located at the atomic site i in a bulk crystal, and $\Phi_{\kappa,i}$ is the local wave function given as the eigenfunction of isolated muffin-tin potential [1,4,5]. The variational basis functions of this Hamiltonian are atomic orbitals $\chi_{lm}(|\mathbf{r}|)=\phi_l(|\mathbf{r}|)Y_{lm}(\theta,\varphi)$, which are given by solving the *Schrödinger* equation for the norm-conserving pseudo-potential

* Corresponding author.

SSDI 0920-5861(94)00151-0

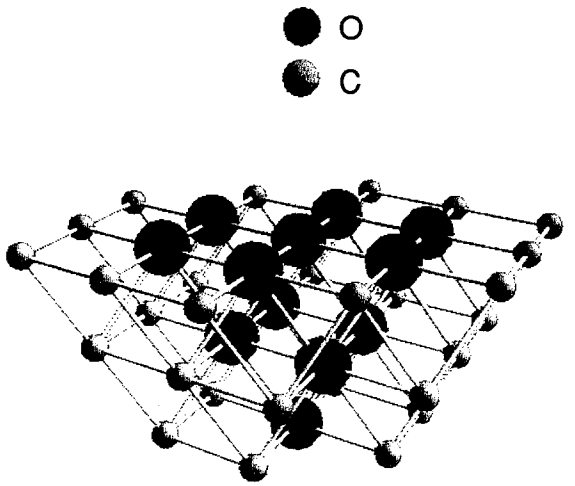

Fig. 1. $W_{12}V_{M28}$–*CO* model cluster for CO/W(110).

self-consistently. The molecular orbital represented by the linear combination of symmetrized orbitals is determined by the standard density functional scheme [3]. The total energy is given by

$$E_{\text{tot}}=\sum_{\nu} f_\nu \epsilon_\nu - \frac{1}{2}\int\int \frac{\rho(\mathbf{r})\rho(\mathbf{r}')}{|\mathbf{r}-\mathbf{r}'|}\mathrm{d}\mathbf{r}\mathrm{d}\mathbf{r}' + E_{\text{XC}} - \int \rho(\mathbf{r}) V_{\text{XC}}(\rho(\mathbf{r}))\mathrm{d}\mathbf{r} + \sum_{i<j}\frac{Z_i Z_j}{|\mathbf{R}_i-\mathbf{R}_j|} \quad (3)$$

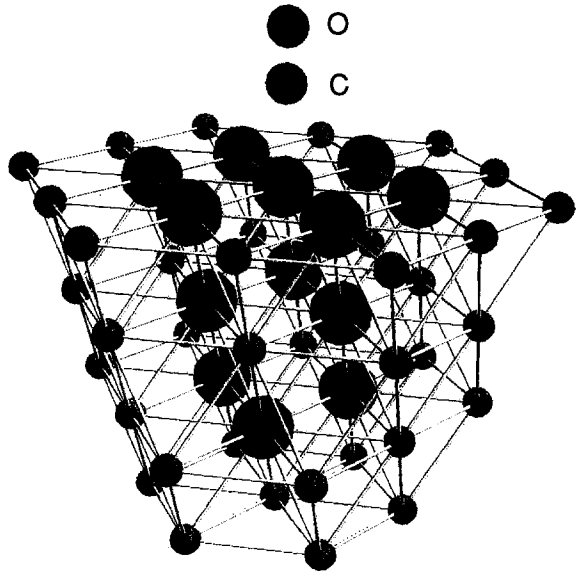

Fig. 2. $Pt_{13}V_{M37}$–*CO* model cluster for CO/Pt(111).

where ε_ν and f_ν are the eigenvalue and occupation number at the eigenstate ν, respectively.

1.2. Poisson equation

The Coulomb energy requires the highest accuracy in determining the total energy of the cluster. In our LCPSAO method, Coulomb potential is calculated by dividing the total charge density into nonspherical atom-like ones, $\rho_{ilm}(\mathbf{r}_i)$, located in each atomic site,

$$\rho(\mathbf{r}) = \sum_{ilm}\rho_{ilm}(\mathbf{r}_i) = \sum_{ilm}\rho_{ilm}(r_i)Y_{lm}(\mathbf{r}_i) \quad (4)$$

where $r_i \equiv |\mathbf{r}-\mathbf{R}_i|$. $\rho_{ilm}(\mathbf{r}_i)$ is roughly determined by the standard fitting procedure using charge density basis functions as

$$\rho_{ilm}(\mathbf{r}_i) \simeq \sum_{kl'l''j} q_{kl'l''j}\phi_{klmj}(r_i)Y_{lm}(\mathbf{r}_i) \quad (5)$$

$$\phi_{klmj}(r_i) = \chi_{l'}(r_i)\chi_{l''}(r_i)f_j(r_i) \quad (6)$$

where $\chi_l(r_i)$ is the radial wave function of atomic orbital and the pairs of (l',l'') are given by taking all possible combinations associated with l. f_j is the auxiliary function to increase number of fitting basis functions. After getting rough convergence of the LCPSAO self-consistent procedure, the Coulomb potential is accurately calculated by the numerical multi-expansion method by applying Becke's fuzzy-cell decomposition scheme for multicenter numerical integration [4].

$$\rho_{ilm}(r_i) = \int \rho(\mathbf{r}) w_i(\mathbf{r}) Y_{lm}(\mathbf{r}_i)\mathrm{d}\Omega_i \quad (7)$$

$w_i(\mathbf{r})$ is the weight of fuzzy-cell located at site i. ρ_{ilm} is updated in every iteration and the Poisson equation for each lm is solved by the one dimensional radial numerial integrations. The total Coulomb potential is given by superimposing atom-like Coulomb potentials from each site.

1.3. Models

Figs. 1 and 2 show the geometrical configuration of model clusters of $CO/W_{12}V_{M28}$ for CO/

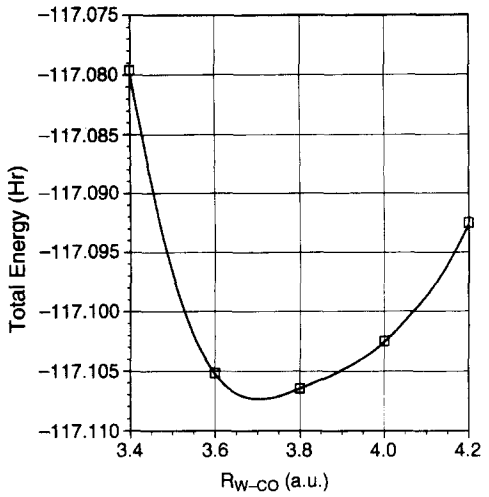

Fig. 3. Total energy of $W_{12}V_{M28}$–CO vs. W–C bond length.

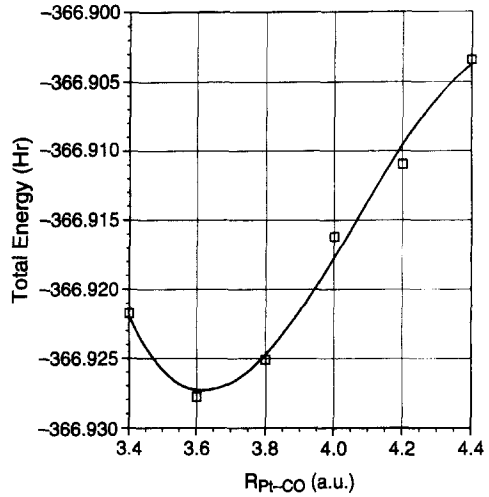

Fig. 4. Total energy of $Pt_{13}V_{M37}$–CO vs. Pt–C bond length.

W(110) and $CO/Pt_{13}V_{M37}$ for CO/Pt(111), respectively. Bond lengths of Pt–Pt, Pt–V_M, V_M–V_M are kept fixed at the bulk value, 5.2423 in atomic unit (a.u.). Tungsten(110) forms an elongated hexagonal plate layer with the nearest neighbor at 5.165 a.u. and plate distance of 4.217 a.u., which are also taken from bulk constants. It is known that CO is adsorbed on the top site of Pt(111) with the molecular axis perpendicular to the surface and the carbon atom nearest to the surface [6]. On W(110), there are many possible configurations of adsorbate such as liner, bridge, vertical, and horizontal. For comparison we adopted the vertical and on-top configurations. The muffin-tin radii used to calculate the model potential are 2.945 a.u. (W) and 2.897 a.u. (Pt). In the cases of NO adsorption, C atoms of these models are replaced by N atoms. Unless otherwise designated, both C–O and N–O distances are fixed at gas phase values, 2.132 a.u. and 2.175 a.u., respectively.

2. Results and discussions

2.1. Total energy

Figs. 3–6 show the total energy curves of W_{12}–CO, Pt_{13}–CO, W_{12}–NO and Pt_{13}–NO vs. metal–

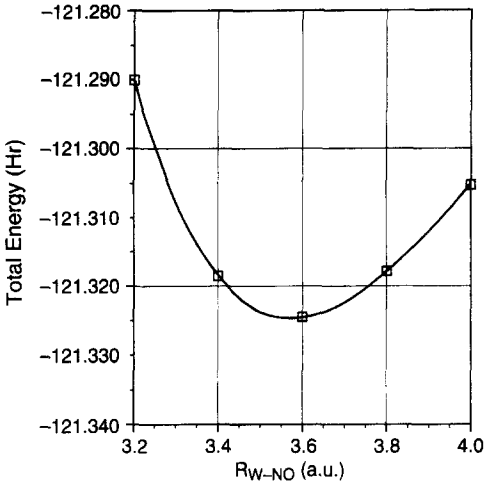

Fig. 5. Total energy of $W_{12}V_{M28}$–NO vs. W–N bond length.

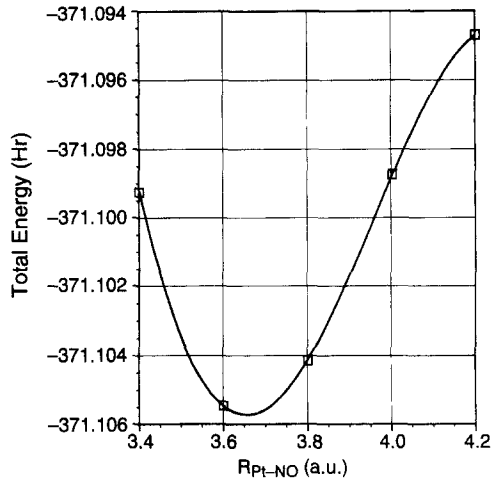

Fig. 6. Total energy of $Pt_{13}V_{M37}$–NO vs. Pt–N bond length.

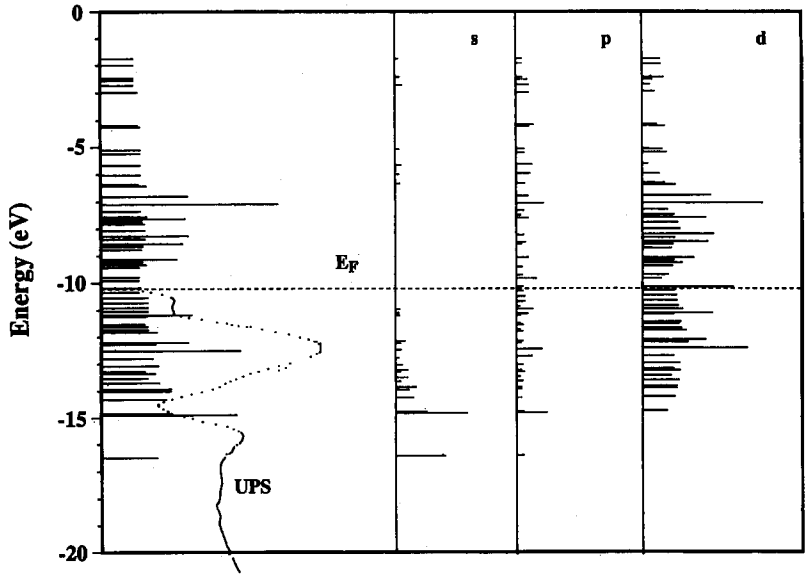

Fig. 7. LDOS of $W_{12}V_{M28}$ cluster and UPS of W(110).

CO (or NO) bond length. The equilibrium distances of metal–C (or N) are 3.80 a.u. (CO/W), 3.57 a.u. (NO/W), 3.62 a.u. (CO/Pt) and 3.64 a.u. (NO/Pt). The calculated binding energies on fixed adsorbate bond lengths are 86 kcal/mol (CO/W), 44 kcal/mol (CO/Pt), 39 kcal/mol (NO/Pt), and 107 kcal/mol (NO/W). Experimental values by thermal desorption (TD) measurement are 50–80 kcal/mol (CO/W(110)) [7], 33 kcal/mol (CO/Pt(111)) [8], 25 kcal/mol (NO/Pt(111)) [9]. Since it is known that NO adsorbs on the Pt surface molecularly and adsorbs on the W surface dissociatively, calculated binding energies are in good agreement with experimental ones. The metal–CO stretching frequencies estimated from the second derivative of the total energy curve, are 487 cm^{-1} and 423 cm^{-1} for W(110) and Pt(111), respectively.

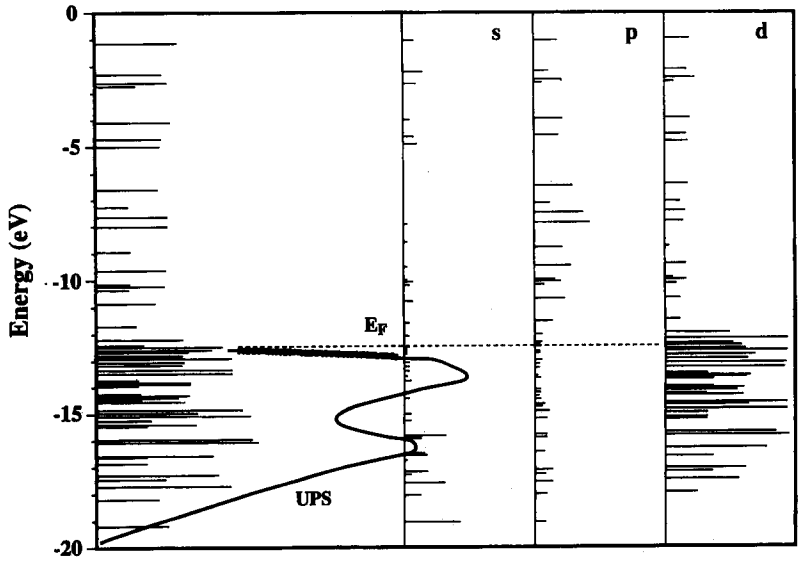

Fig. 8. LDOS of $Pt_{13}V_{M37}$ cluster and UPS of Pt(111).

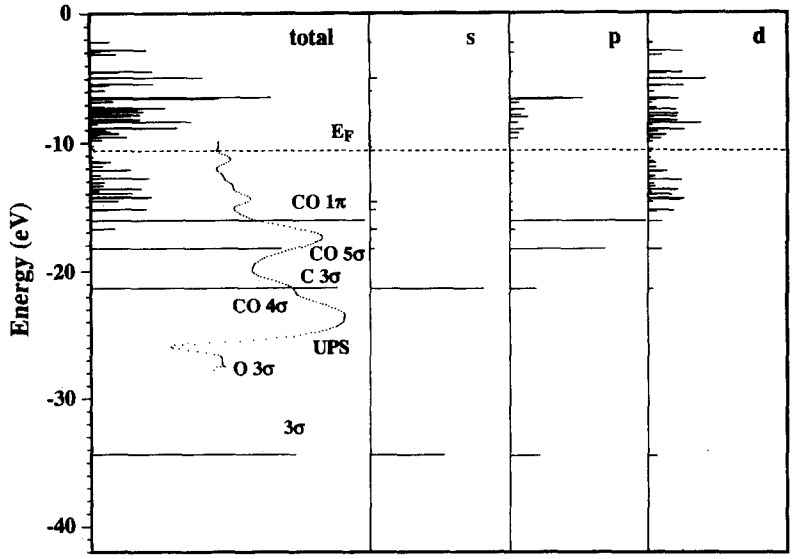

Fig. 9. LDOS of C and W sites of $W_{12}V_{M28}$–*CO* cluster and UPS of CO/W(110).

They agree quite well with experimental values, 403 cm^{-1} and 468 cm^{-1}, respectively [10,11]. The metal–NO stretching frequencies calculated by the same procedure are 565 cm^{-1} (NO/W) and 392 cm^{-1} (NO/Pt). The experimental value for NO/Pt(100) is 230 cm^{-1}–465 cm^{-1} [12].

2.2. *Electronic structure*

Figs. 7 and 8 are local density of states (LDOS) of W_{12} and Pt_{13} with experimental ultraviolet photoelectron spectroscopy (UPS) data [13,14]. The LDOS is calculated as the sum of density of states within muffin-tin radius of each cluster atom. The LDOS above the tungsten Fermi level is crowded while those of platinum are sparse. LDOS's of C and W of CO/W(110), C of CO/Pt(111), N and W of NO/W(110), and N and Pt of NO/Pt(111) clusters are shown in Figs. 9–12 with UPS [13–16] data, respectively. The quote UP spectra are the difference curves between clean metal sur-

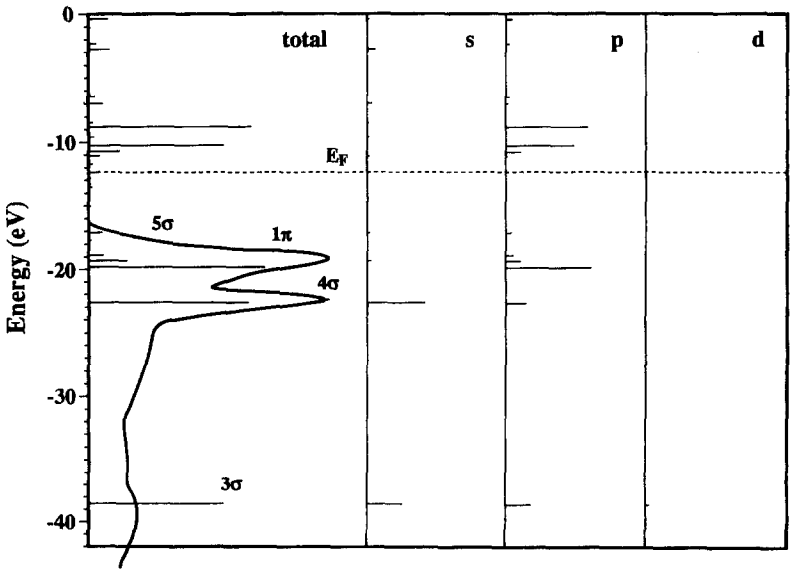

Fig. 10. LDOS of C site of $Pt_{13}V_{M37}$–*CO* cluster and UPS of CO/Pt(111).

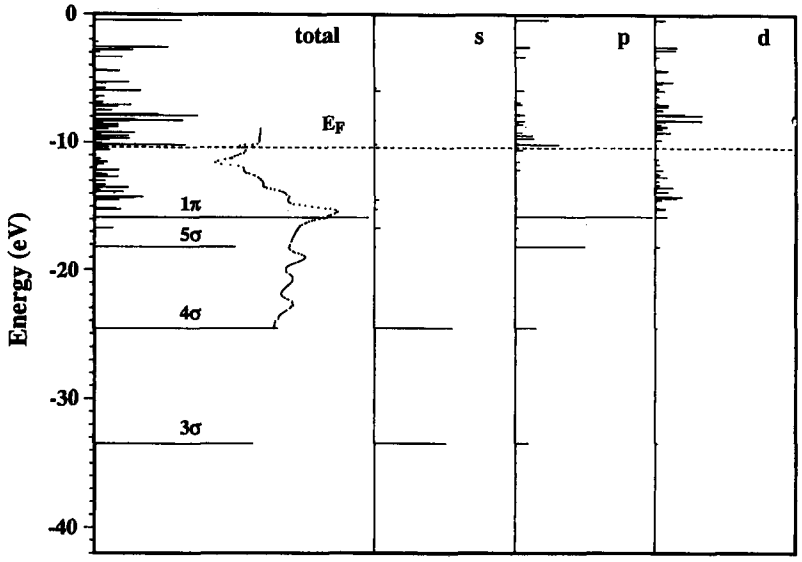

Fig. 11. LDOS of N and W sites of $W_{12}V_{M28}$–*NO* cluster.

faces and CO or NO adsorbed surfaces. LDOS's are given for systems at fixed equilibrium distances: 3.8 a.u. for CO/W and 3.6 a.u. for CO/Pt, NO/W, and NO/Pt. In the case of CO/Pt, the calculated DOS of the C site agrees very well with the UPS data, while for the other systems the LDOS of the metal site and the C or N site seems to be in better agreement with UPS. The adsorption does not perturb metal states so much in the CO/Pt system. It may be due to the partial decomposition of CO or NO on the W surface.

2.3. *Mulliken charge*

The Mulliken population analysis in our LCPSAO SCF scheme is summarized in Tables 1 and 2. Charge transfers from metals to adsorbates at the equilibrium distances are about 0.3 electron

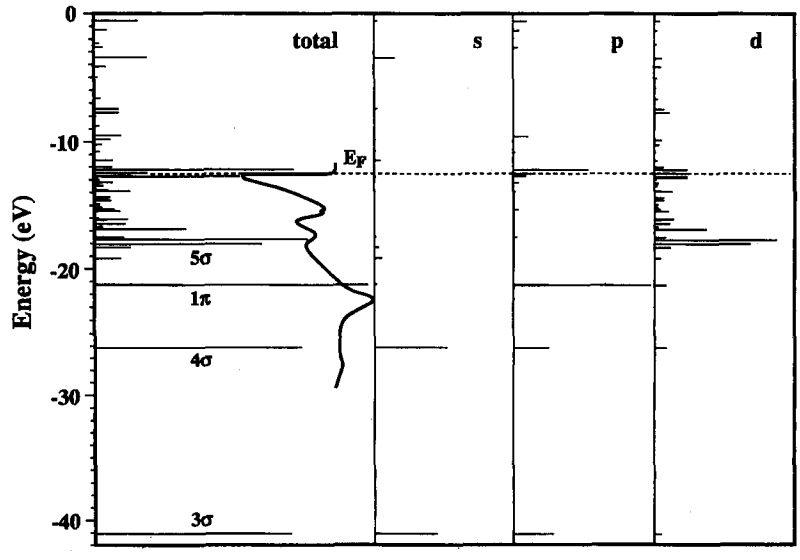

Fig. 12. LDOS of N and Pt sites of $Pt_{13}V_{M37}$–*NO* cluster.

Table 1
Mulliken charges of $W_{12}CO$ and $Pt_{13}CO$ at metal(M)–CO equilibrium distance. Metal site at the center of cluster surface, C site, O site and the sum of C site and O site charges are indicated

R_{M-CO} (a.u.)	M	C	O	CO
W–CO ($R=3.8$)	5.82	4.04	6.28	10.32
Pt–CO ($R=3.6$)	9.88	3.87	6.23	10.10

Table 2
Mulliken charges of $W_{12}NO$ and $Pt_{13}NO$ at metal(M)–NO equilibrium distance. Metal site at the center of cluster surface, N site, O site and the sum of N site and O site charges are indicated

R_{M-CO} (a.u.)	M	N	O	NO
W–NO ($R=3.6$)	5.80	5.25	6.09	11.34
Pt–NO ($R=3.6$)	9.87	5.10	6.01	11.11

for W and 0.1 electron for Pt systems. The difference of 0.2 electron is considered to be large enough to contribute to make CO or NO dissociate on the W surface. These extra charges are in the O site for CO and in the N site for NO.

3. Conclusion

The differences of W and Pt are: (1) d-electron band over Fermi exists on W and d-electron band exists only under Fermi on Pt, (2) the quantity of charge transfer on W is larger than that on Pt. The wide d-band of tungsten is thought to cause the hybridization of adsorbate–p components and the decomposition of adsorbate.

References

[1] S. Ohnishi and N. Watari, Phys. Rev. B, 49 (1994) 14619; S. Ohnishi, T. Ikeda and N. Watari, Computer Aided Innovation of New Materials, North-Holland, Amsterdam, 1991, p. 175.
[2] G.B. Bachelet, D.R. Hamann and M. Schluter, Phys. Rev., B26 (1982) 4299.
[3] P. Hohenberg and W. Kohn, Phys. Rev., 864 (1964) B136; W. Kohn and L.J. Sham, Phys. Rev., 140 (1965) A1133.
[4] A.D. Becke, J. Chem. Phys., 88 (1988) 60; A.D. Becke and R.M. Dickson, J. Chem. Phys., 89 (1988) 2993.
[5] S. Ohnishi, in A. Yoshinori, T. Shinjo and H. Watanabe (Editors), Ordering at Surfaces and Interfaces, Springer Series in Materials Science, Vol. 17, Springer, Berlin, 1992, p. 353.
[6] A.M. Baro and H. Ibach, J. Chem. Phys., 71 (1979) 4821; P. Hoffmann, S.R. Bare, N.V. Richardson and D.A. King, Solid State Commun., 42 (1982) 645.
[7] I. Toyoshima and G.A. Somorjai, Catal. Rev. Sci. Eng., 19 (1979) 105.
[8] S. Ishi, Y. Ohno and B. Viswanathan, Surf. Sci., 161 (1985) 349.
[9] R.J. Gorte, L.D. Schmidt and J.L. Gland, Surf. Sci., 109 (1981) 367.
[10] C. Backx, R.F. Wills, B. Feuerbacher and B. Fitton, Surf. Sci., 63 (1977) 507.
[11] P. Hofmann, S.R. Bare, N.V. Richardson and D.A. King, Solid State Commun., 42 (1982) 645; P.R. Norton, J.W. Goodale and E.B. Belkink, Surf. Sci., 83 (1979) 189; H. Hopster and H. Ibach, Surf. Sci., 77 (1978) 109.
[12] G. Pirung, H.P. Bonzel and H. Ibach, J. Chem. Phys., 71 (1979) 593.
[13] E.W. Plummer, B.J. Waclawski, T.V. Vorburger and C.E. Kuyatt, Progress Surf. Sci., 7 (1976) 147.
[14] J.N. Miller, D.T. Ling, I. Lindau, P.M. Stefan and W.E. Spicer, Phys. Rev. Lett., 38 (1977) 1419.
[15] R.I. Masel, E. Umbach, J.C. Fuggle and D. Menzel, Surf. Sci., 79 (1979) 26.
[16] H.P. Bonzel and G. Pirug, Surf. Sci., 62 (1977) 45.